Platinum-Catalyzed Template Removal for the in Situ Synthesis of MCM-41 Supported Catalysts

Piotr Krawiec,† Emanuel Kockrick,† Paul Simon,‡ Gudrun Auffermann,‡ and Stefan Kaskel*,†

Department of Inorganic Chemistry, Technical University of Dresden, Mommsenstr. 6, D-01062 Dresden, Germany, and Max Planck Institute for Chemical Physics of Solids, Nöthnitzer Str. 40, D-01187 Dresden, Germany

Received December 22, 2005. Revised Manuscript Received March 17, 2006

Platinum-containing MCM-41 was synthesized in a one step approach. In this new procedure, the swelling agent (toluene) was used as a transport medium to inject the Pt precursor, Pt(acetylacetonate)$_2$, directly into the inner core of the surfactant micelles. A 1 wt % metal loading was achieved without the loss of pore ordering, while samples with 2 wt % loading showed a less ordered structure. A total of 80−100% of the Pt precursor was incorporated in the porous host matrix depending on the precursor concentration and final loading. During the calcination process, platinum acts as a catalyst for the oxidative removal of the surfactant molecules, allowing one to decrease the calcination temperature significantly. The calcined material had a high surface area (1000−1200 $m^2\ g^{-1}$). Platinum particles could be detected using transmission electron microscopy confirming also the absence of large particles outside the mesopore system. The in situ approach was also applied to prepare other metal/MCM-41 or oxide/MCM-41 materials such as Pd/MCM-41 and V_2O_5/MCM-41. Both of them showed a high degree of guest incorporation and no significant decrease in surface area. In situ incorporation of metals into SBA-15 resulted in a lower Pt incorporation in the final material (50−60%) and a disordered pore structure, even for low Pt loading (1 wt %). The accessibility of the metallic particles for catalytic reactions was demonstrated using the hydrogenation of cinnamic acid as a model reaction. The highest specific reaction rates were observed for Pd supported on MCM-41 and were comparable to that of commercially available Pd/carbon catalysts.

Introduction

Since the discovery of MCM-41 and MCM-48 by Mobil[1] in 1992, ordered mesoporous silicas were widely studied as supports for catalysts[2,3] or as a matrix for the preparation of nanosized, high surface area materials.[4−7] MCM-41 (Mobil Composition of Matter) not only has a high surface area (up to 1400 $m^2\ g^{-1}$) but also has a narrow pore size distribution (2−6 nm). The advantage of particles confined inside M41S materials is not only the high dispersion of the metal itself but also an increased resistance against sintering[8,9] and, as a consequence, a longer lifetime of the catalyst at high temperature. Typically, Pt supported on MCM-41 is prepared via the wet impregnation of the porous calcined MCM-41 materials with a Pt salt and subsequent reduction to metallic platinum.[10−12] Also the ordered mesoporous silica, SBA-15, with larger pores, was infiltrated with platinum. Shin et al. prepared platinum nanowires[13] inside the pores of ordered mesoporous silica, and more recently Yamada et al.[14] showed how to control the platinum dispersion inside SBA-15 using gamma radiation or thermal treatment resulting in a coating of the walls or nanoparticles inside the pores, respectively. Post-synthetic functionalization of the silica surface followed by ion exchange has also been used by Yang et al. to prepare metal containing mesostructured silica.[15,16] Separately prepared platinum nanoparticles were injected into the SBA-15 pores by sonication[17] or directly during the synthesis in a two step procedure.[18] This synthesis approach was proposed also for MCM-41, in which Pt nanoparticles are first

* To whom correspondence should be addressed. Phone: +49-3514633-4885. Fax: +49-35104633-7287. E-mail: stefan.kaskel@chemie.tu-dresden.de.
† Technical University of Dresden.
‡ Max Planck Institute for Chemical Physics of Solids.

(1) Kresge, C. T.; Leonowicz, M. E.; Roth, W. J.; Vartuli, J. C.; Beck, J. S. *Nature* **1992**, *359*, 710−712.
(2) Taguchi, A.; Schüth, F. *Microporous Mesoporous Mater.* **2005**, *77*, 1−45.
(3) Sauer, J.; Kaskel, S.; Janicke, M.; Schüth, F. *Stud. Surf. Sci. Catal.* **2001**, *135*, 4740−4747.
(4) Schüth, F. *Chem. Mater.* **2001**, *13*, 3184−3195.
(5) Krawiec, P.; Weidenthaler, C.; Kaskel, S. *Chem. Mater.* **2004**, *16*, 2869−2880.
(6) Ryoo, R.; Joo, S. H.; Kruk, M.; Jaroniec, M. *Adv. Mater.* **2001**, *13*, 677−681.
(7) Dibandjo, P.; Bois, L.; Chassagneux, F.; Cornu, D.; Letoffe, J. M.; Toury, B.; Babonneau, F.; Miele, P. *Adv. Mater.* **2005**, *17*, 571−574.
(8) Zhang, L.; Papaefthymiou, G. C.; Ying, J. Y. *J. Phys. Chem. B* **2001**, *105*, 7414−7423.
(9) Molnar, E.; Konya, Z.; Kiricsi, I. *J. Therm. Anal. Calorim.* **2005**, *79*, 573−577.
(10) Yao, N. S.; Pinckney, C.; Lim, S. Y.; Pak, C.; Haller, G. L. *Microporous Mesoporous Mater.* **2001**, *44*, 377−384.
(11) Jentys, A.; Schiesser, W.; Vinek, H. *Catal. Today* **2000**, *59*, 313−321.
(12) Junges, U.; Jacobs, W.; Voigtmartin, I.; Krutzsch, B.; Schüth, F. *J. Chem. Soc., Chem. Commun.* **1995**, 2283−2284.
(13) Shin, H. J.; Ko, C. H.; Ryoo, R. *J. Mater. Chem.* **2001**, *11*, 260−261.
(14) Yamada, T.; Zhou, H. S.; Hiroishi, D.; Tomita, M.; Ueno, Y.; Asai, K.; Honma, I. *Adv. Mater.* **2003**, *15*, 511−513.
(15) Yang, C. M.; Liu, P. H.; Ho, Y. F.; Chiu, C. Y.; Chao, K. J. *Chem. Mater.* **2003**, *15*, 275−280.
(16) Yang, C. M.; Sheu, H. S.; Chao, K. J. *Adv. Funct. Mater.* **2002**, *12*, 143−148.
(17) Rioux, R. M.; Song, H.; Hoefelmeyer, J. D.; Yang, P.; Somorjai, G. A. *J. Phys. Chem. B* **2005**, *109*, 2192−2202.

10.1021/cm052830n CCC: $33.50
Published on Web 05/04/2006

Scheme 1. Schematic Illustration of the in Situ Pt/MCM-41 Preparation (See Text)

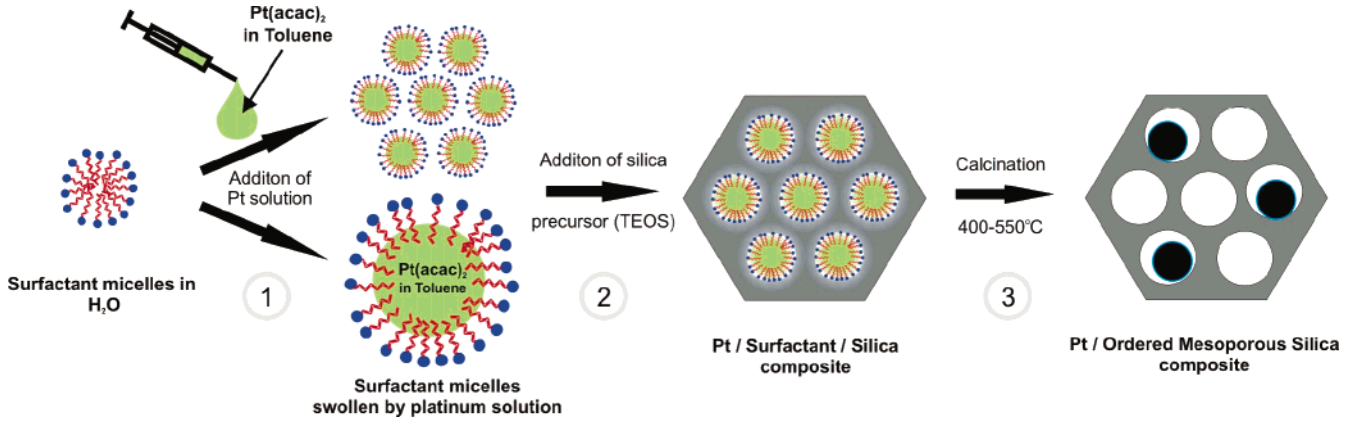

prepared in solution and subsequently incorporated into porous silica within the synthesis.[18−20] Both procedures require multiple steps during the preparation and long synthesis times. A more straightforward method is to dissolve the metal precursor in the aqueous phase of the surfactant solution from which mesoporous silica is synthesized. However, in this case only a low amount of platinum can be incorporated in the porous host material, while more than 20%[12] or 40%[21,22] remains in solution and large platinum particles are also detected outside the pores.[12] In this work, we present a new approach to prepare well-dispersed platinum nanoparticles predominately inside the pores of MCM-41 in one step. In this method, a solution of a platinum precursor in a hydrophobic, nonpolar solvent [Pt(acetylacetonate)$_2$ (Pt(acac)$_2$) in toluene] is used and injected inside the hydrophobic core of the surfactant micelles used as the template for the MCM-41 structure, before addition of the silica source (Scheme 1, step 1). Because both Pt(acac)$_2$ and toluene do not mix with water, they will be dissolved in the inner hydrophobic core of the micelles, resulting in a high degree of incorporation. Thus, 80−100% of the precursor are incorporated in the final material. In the as-synthesized platinum containing MCM-41, surfactant removal is catalytically enhanced as a result of the presence of platinum resulting in a lower calcination temperature needed as compared to pure MCM-41.[23,24] Catalytic template removal was also observed by Montes et al.[25] who added platinum to the as-synthesized MCM-41 material before calcination. The method presented here is widely applicable to other metal containing silica systems such as Pd/MCM-41, V_2O_5/MCM-41, and Pt/SBA-15, using the same procedure and acetylacetonates as precursors. Not only was palladium-loaded MCM-41 found to be a good hydrogenation catalyst in the cinnamic acid hydrogenation, but also vanadium containing silica is a promising catalyst in a number of reactions.[26−28]

Experimental Section

Pt/MCM-41 Synthesis Procedure. A somewhat modified synthesis of Grün et al.[29,30] was employed. A total of 1.2 g CTABr (cetyltrimethylammonium bromide; 99%; Acros) was dissolved in 60 mL of H_2O and 4.75 g of concentrated NH_3 (25%) and heated to 50 °C. The solution was kept in a closed glass bottle during the synthesis. To this mixture was added an appropriate amount of Pt(acac)$_2$ dissolved in toluene (the Pt(acac)$_2$ solutions were ultrasonicated at 80 °C and added quickly before cooling down). The resulting mixture was stirred rigorously for 20 min at 50 °C, and 5 g of TEOS (tetraethylorthosilicate; 98%; Acros) was added at once. The mixture was subsequently stirred for another 60 min and cooled to 35 °C, and the solid was filtered out and washed with 100 mL of distilled water. The solid product was dried at 100 °C overnight and calcined in air according to the following heating program: heating to 180 °C at 1 °C min^{-1} with a plateau for 180 min at 180 °C and heating to 450 °C at 1 °C min^{-1}, followed by a plateau at 450 °C for 5 h. For the synthesis of Pd/MCM-41 and V_2O_5/MCM-41 instead of Pt(acac)$_2$, Pd(acac)$_2$ in toluene was used as a metal precursor for palladium containing MCM-41 materials, and V(acac)$_3$ in toluene was used for vanadium integration in MCM-41.

Pt/SBA-15. For metal-containing SBA-15 the synthesis method of Zhao et al.[31,32] was modified. A total of 2.41 g of Pluronic 123 (BASF) were dissolved in 63.4 g of distilled water (overnight) and 12.05 mL of HCl (37%). Subsequently, an appropriate amount of the Pt(acac)$_2$/toluene solution was added (at 40 °C) and stirred for 20 min. In the next step, 5 g of TEOS were added within 30 min (while stirring) and stirred for 4 h at the same temperature. An additional heat treatment at 80 °C in a polypropylene bottle was

(18) Zhu, J.; Konya, Z.; Puntes, V. F.; Kiricsi, I.; Miao, C. X.; Ager, J. W.; Alivisatos, A. P.; Somorjai, G. A. *Langmuir* **2003**, *19*, 4396−4401.
(19) Lin, K. J.; Chen, L. J.; Prasad, M. R.; Cheng, C. Y. *Adv. Mater.* **2004**, *16*, 1845−1848.
(20) Konya, Z.; Puntes, V. F.; Kiricsi, I.; Zhu, J.; Alivisatos, P.; Somorjai, G. A. *Catal. Lett.* **2002**, *81*, 137−140.
(21) Aramendia, M. A.; Borau, V.; Jimenez, C.; Marinas, J. M.; Romero, F. J. *Chem. Commun.* **1999**, 873−874.
(22) Chatterjee, M.; Iwasaki, T.; Onodera, Y.; Nagase, T. *Catal. Lett.* **1999**, *61*, 199−202.
(23) Kleitz, F.; Schmidt, W.; Schüth, F. *Microporous Mesoporous Mater.* **2003**, *65*, 1−29.
(24) Keene, M. T. J.; Gougeon, R. D. M.; Denoyel, R.; Harris, R. K.; Rouquerol, J.; Llewellyn, P. L. *J. Mater. Chem.* **1999**, *9*, 2843−2850.
(25) Montes, A.; Cosenza, E.; Giannetto, G.; Urquieta, E.; de Melo, R. A.; Gnep, N. S.; Guisnet, M. *Stud. Surf. Sci. Catal.* **1998**, *117*, 237.
(26) Fornes, V.; Lopez, C.; Lopez, H. H.; Martinez, A. *Appl. Catal., A* **2003**, *249*, 345−354.
(27) Shylesh, S.; Singh, A. P. *J. Catal.* **2004**, *228*, 333−346.
(28) George, J.; Shylesh, S.; Singh, A. P. *Appl. Catal., A* **2005**, *290*, 148−158.
(29) Grün, M.; Lauer, I.; Unger, K. K. *Adv. Mater.* **1997**, *9*, 254.
(30) Grün, M.; Unger, K. K.; Matsumoto, A.; Tsutsumi, K. *Microporous Mesoporous Mater.* **1999**, *27*, 207−216.
(31) Zhao, D. Y.; Feng, J. L.; Huo, Q. S.; Melosh, N.; Fredrickson, G. H.; Chmelka, B. F.; Stucky, G. D. *Science* **1998**, *279*, 548−552.
(32) Zhao, D. Y.; Huo, Q. S.; Feng, J. L.; Chmelka, B. F.; Stucky, G. D. *J. Am. Chem. Soc.* **1998**, *120*, 6024−6036.

performed without stirring for 24 h. The solution was cooled, filtrated, washed with 100 mL of water, dried at 100 °C, and calcined using the same temperature program as indicated for the Pt/MCM-41 synthesis.

Hydrogenation of Cinnamic Acid. A total of 0.4 g of cinnamic acid (99%; Aldrich) were dissolved in 16 g of ethanol (99%). To the substrate was added 0.24 g of the solid catalyst. The mixture was stirred, and dynamic hydrogen was used for the reduction (1 bar, 50 mL min^{-1}) without any pretreatment of the catalyst. Periodically taken samples were analyzed with a GC/MS (Shimadzu GCMS-QP5000). For comparison, the reaction was also carried out using a commercially available Pd/carbon catalyst with the same substrate/catalyst ratio (5 wt % Pd, Escat 103; Aldrich), which is later referred to as C-1.

Characterization. X-ray powder diffraction patterns were recorded in transmission geometry using a Stoe Stadi-P diffractometer and Cu $K\alpha_1$ radiation ($\lambda = 0.15405$ nm).

The nitrogen physisorption isotherms were measured at −196 °C using a Quantachrome Autosorb 1C apparatus. Prior to the measurement, the samples were evacuated at 150 °C for 5 h. Specific surface areas were calculated using the BET equation in a relative pressure range between $P/P_0 = 0.05-0.2$. The pore size distribution was estimated from the desorption branch of the isotherm using the BJH method assuming a cylindrical pore model.

The chemical analyses of the content of platinum, palladium, and vanadium, respectively, were carried out with an ICP-OES (inductively coupled plasma−optical emission spectrometer) Vista (Varian). The samples (amount of about 10 mg) were digested in a mixture of 1.5 mL of HCl (37%), 0.5 mL of HNO_3 (65%), and 1 mL of HF (40%) by heating. Generally, the solutions were diluted to a volume of 50 mL using a volumetric flask.

For transmission electron microscopy (TEM) investigations, Pt/MCM-41 powder was suspended in ethanol and one drop of the suspension was placed on a carbon film coated copper grid. After drying, TEM micrographs were obtained using a Philips CM200 FEG\ST Lorentz electron microscope with a field emission gun at an acceleration voltage of 200 kV. TEM investigations were carried out at the Triebenberg Laboratory for High-Resolution Electron Microscopy and Holography, Technical University of Dresden, Germany.

The thermogravimetry (TG)/MS measurements were carried out using a Netzsch STA 409PC thermobalance coupled with a Netzsch QMS 403C mass spectrometer via a capillary heated to 300 °C. Samples were heated in air up to 700 °C with a heating rate of 2 °C min^{-1}.

Results and Discussion

In Situ Pt Incorporation into MCM-41 Materials. In a typical synthesis procedure, a solution of CTABr (surfactant) in H_2O and NH_3 was used. Subsequently, appropriate amounts of Pt(II)acetylacetonate in toluene (Table 1) were added (Scheme 1, step 1). After adding TEOS (Scheme 1, step 2) the solid was isolated by filtration, washed with water, and calcined at 450 °C (Scheme 1, step 3). The choice of $Pt(acac)_2$ as a precursor and toluene as the swelling agent is not arbitrary. As a result of the lack of solubility in water, $Pt(acac)_2$ preferentially dissolves in the toluene phase. On the other hand, toluene can dissolve reasonably high amounts of this Pt precursor (up to 3.2 wt % at 70 °C) and also does not mix with water. In this approach (depending on the loading and precursor concentration) 80−100% of the platinum is incorporated into MCM-41 (Table 1), avoiding losses of this expensive metal during the synthesis. For highly saturated solutions of the precursor, a lower platinum incorporation is observed (Table 1, M-2 and M-4), while for the more diluted solution of $Pt(acac)_2$ (M-3) and lower loading (M-1) almost all platinum is incorporated. The latter can be due to the presence of ethanol in the solution after addition of TEOS. Ethanol increases the solubility of $Pt(acac)_2$ outside the micelles and, therefore, causes leaching of the metal complex. The volume of the $Pt(acac)_2$/toluene solution that can be solubilized by CTABr micelles is limited. Higher loadings (2 wt %, M-4 sample) also cause a decrease in pore ordering. The latter is clearly visible in low angle X-ray diffractograms (Figure 1a). For sample M-4 with 2 wt % Pt, only one broad (100) peak could be observed and the (110) and (200) reflections disappeared. However, in the case of 1 wt % loading of platinum (M1) no loss of the ordering was observed as compared to pure MCM-41 and three reflections of the hexagonal structure are discerned. Increasing the Pt/toluene loading also causes a significant increase of the (100) lattice spacing as expected for the addition of swelling agents.[33] TEM micrographs further confirm this

Table 1. Synthesis Conditions and Characterization of Platinum Containing MCM-41 Materials

sample code		amount of Pt solution added[a] [mL]	theroretical/ measured Pt loading [wt %]	Pt yield[e] [%]	surface area [$m^2\ g^{-1}$]
M-0	MCM-41				1189
M-1	0.4 wt % Pt	0.4[b]	0.39/0.39	100	1190
M-2	1 wt % Pt	1[c]	0.99/0.79	80	1126
M-3	1 wt % Pt	2[d]	0.99/0.86	87	1098
M-4	2 wt % Pt	2[c]	1.97/1.69	86	1073

[a] Per 1.2 g of CTABr and 5 g of TEOS used. [b] 2.4 wt % $Pt(acac)_2$ in toluene solution was used. [c] 3.2 wt % $Pt(acac)_2$ in toluene solution was used. [d] 1.6 wt % $Pt(acac)_2$ in toluene solution was used. [e] Pt yield determined using the ICP-OES.

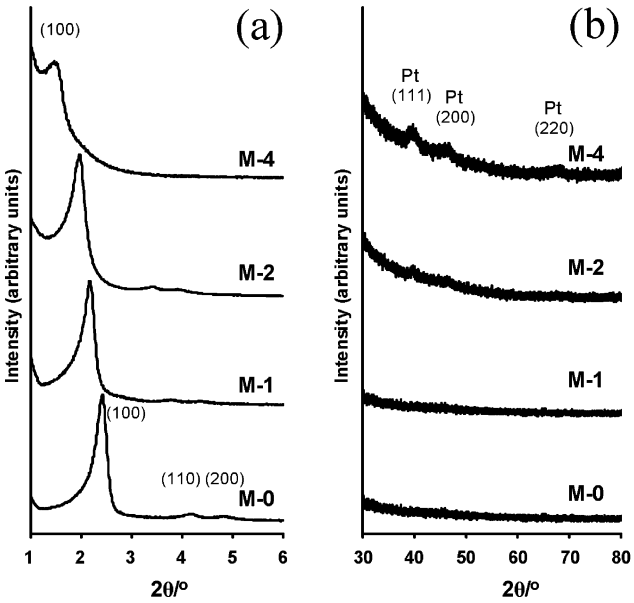

Figure 1. (a) Low and (b) high angle XRD of Pt/MCM-41 samples. M-0 is a pure MCM-41, while M-1, M-2, and M-4 are Pt/MCM-41 materials with different metal loading (Table 1). The presence of nanocrystalline Pt was detected for M-4 and M-2.

(33) Lind, A.; Andersson, J.; Karlsson, S.; Agren, P.; Bussian, P.; Amenitsch, H.; Linden, M. *Langmuir* **2002**, *18*, 1380−1385.

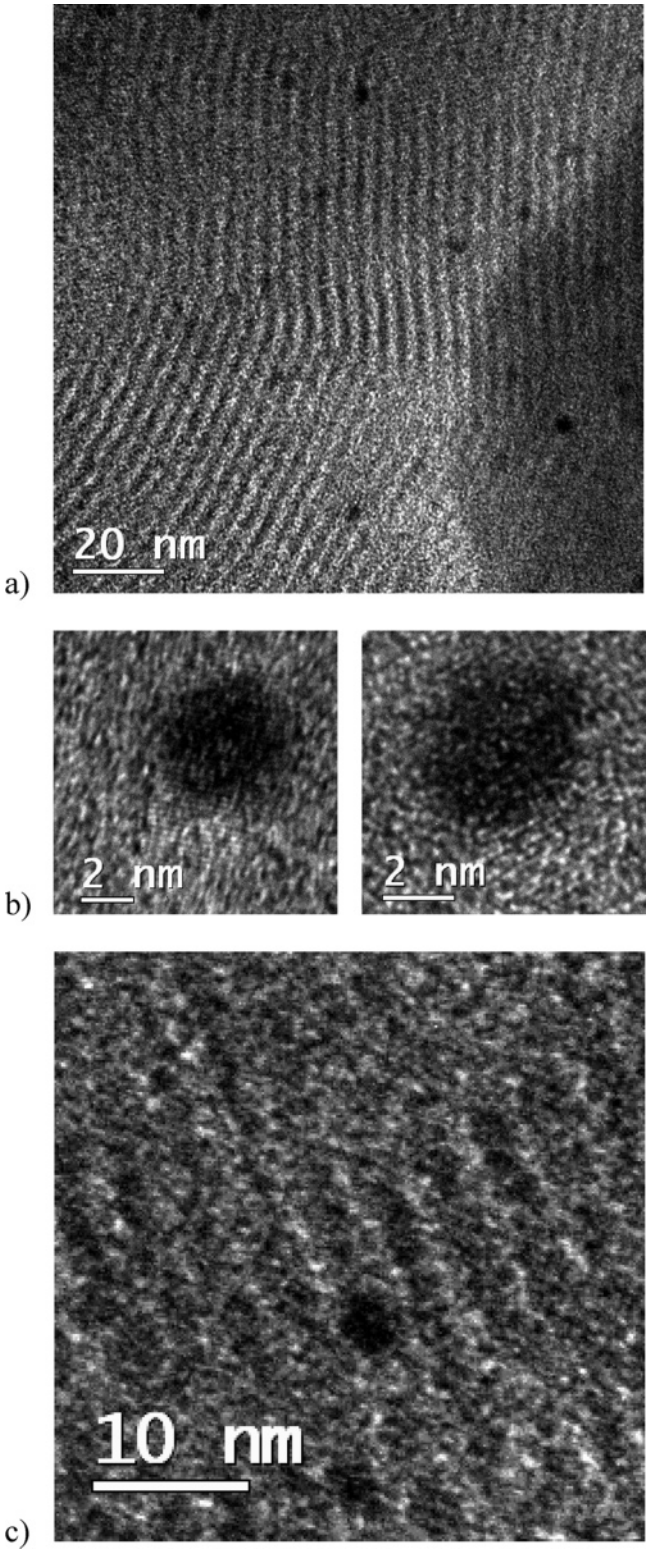

Figure 2. (a) Overview TEM micrograph of sample M-2 with 1 wt % Pt/MCM-41. Platinum particles (dark) are statistically embedded within bent silica pore walls (periodicity ~ 3.9 nm). High-resolution TEM micrographs of M-2 displaying a single platinum nanoparticle with (111) lattice fringes corresponding to about 2.24 Å. (c) Magnified image of a single nanoparticle integrated in the nanoporous host. Bending of the SiO_2 pore wall is caused by stress induced at the built-in area.

conclusion. Comparing Figures 2a and 3a, ordering of the pores in sample M-2 is significantly better than that of M-4 (Figure 3a). The micrographs also show the incorporated Pt nanoparticles (dark spots) inside the channels of MCM-41,

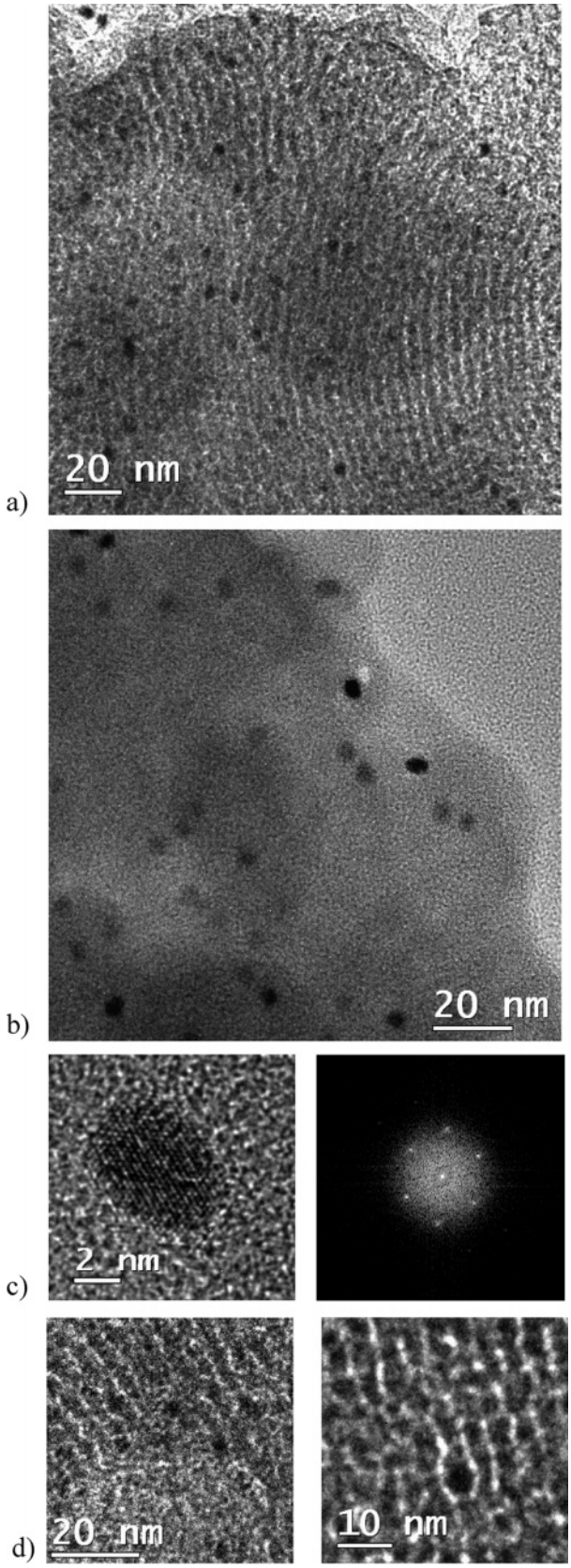

Figure 3. (a) Defocused overview TEM image of sample M-4 with 2 wt % Pt/MCM-41 and a periodicity of about 4.4 nm. (b) In-focus overview TEM image of sample M-4 with 2 wt % Pt/MCM-41. Under in-focus conditions only platinum nanoparticles are visible. (c) High-resolution TEM micrograph and its fast Fourier transform (FFT) of M-4 displaying a single Pt nanoparticle with (111) and (200) lattice fringes corresponding to about 2.27 and 1.92 Å. (d) Magnified image of incorporated platinum nanoparticles. Bending of the SiO_2 wall is caused by stress induced at the built-in area.

Table 2. Synthesis Conditions and Characterization of Mesoporous Composite Materials[a]

sample code		amount of metal solution added [mL]	theroretical/ measured metal loading[f] [wt %]	metal yield[f] [%]	surface area [m^2 g^{-1}]
S-0	SBA-15		0		786
S-1	1 wt % Pt	1[b]	0.99/0.48	48	825
S-2	2 wt % Pt	2[b]	1.99/1.17	59	824
V-1	1.4 wt % V	1[c]	1.39/1.33	96	1187
V-2	1.4 wt % V	*d*	1.39/1.13	81	1056
P-1	0.3 wt % Pd	1.8[e]	0.34/0.30	88	1100

[a] Pure SBA-15 (S-0) and platinum incorporated SBA-15 samples are marked as samples S-1 and S-2. Vanadium (V-1 and V-2) and palladium (P-1) containing MCM-41 materials are also listed. [b] Per 2.41 g of P123 block copolymer and 5 g of TEOS used. 3.2 wt % $Pt(acac)_2$ solution in toluene was added. [c] Per 1.2 g of CTABr and 5 g of TEOS used. As the vanadium source, 13.8 wt % $V(acac)_3$ solution in toluene was added. [d] 0.14 g of $V(acac)_3$ added directly to water/surfactant mixture before synthesis, without toluene. [e] 1.8 wt % $Pd(acac)_2$ solution in toluene was added. [f] Metal loading after synthesis was confirmed by ICP-OES.

and no large particles outside were found. The average particle size was estimated to be 3.0 nm in the case of M-2 (Figure 2b) and 4.17 nm in the case of M-4 (Figure 3b). These values are in good agreement with the measured pore diameter of the silica matrix calculated from nitrogen physisorption isotherms measured at 77 K (3.3 nm pore diameter for 1 wt % Pt sample (M2) and 3.7 nm pore diameter for 2 wt % Pt sample (M4)—BJH desorption—see Supporting Information). No significant decrease in the surface area as compared to standard MCM-41 (1190 m^2 g^{-1}) was observed in all Pt/MCM-41 samples. For the sample with the highest 2 wt % Pt loading, a surface area of 1073 m^2 g^{-1} was measured. Wide-angle X-ray diffractograms show the presence of the cubic metallic platinum in samples with high Pt loading (Figure 1b). The reduction to Pt^0 is also confirmed in the X-ray photoelectron spectroscopy (XPS) spectra (Pt $4f_{7/2}$, 70.5 eV).[34]

In Situ Synthesis of Pd/MCM-41, Pt/SBA-15, and V_2O_5/MCM-41. The general method of injecting the hydrophobic platinum precursor into micelles during the synthesis of MCM-41 materials can be extended to other metals (Pd, V) and other ordered mesoporous materials such as SBA-15. In the original synthesis scheme, $Pt(acac)_2$ is replaced by $Pd(acac)_2$ (Scheme 1, step 1), and Pd/MCM-41 can be made according to the same procedure (Scheme 1). The acetylacetonate of palladium is also insoluble in water, and injection using a toluene solution results in 88% of metal incorporation (Table 2, sample P-1]. On the other hand, less palladium can be dissolved in toluene (1.8 wt % at 70 °C) and loading of the final composite material is generally lower (0.3 wt %). Another example can be the incorporation of vanadium. In this case $V(acac)_3$ can be used as a precursor. However, this compound also dissolves in water. Thus a direct comparison was made using the precursor dissolved in toluene (V-1) and in the surfactant solution with water (V-2; Table 2). For sample V-1, the vanadium precursor was dissolved in toluene and a high incorporation of vanadium (96%) was measured after the synthesis. However, solubilization of the same vanadium precursor in water (sample V-2) resulted in an incorporation as high as 81%. This is due to the nature of vanadium which, in contrast to platinum, can integrate into the silica network, even for low concentrated solutions.[28,35−37]

On the other hand, incorporation of platinum into the pores of SBA-15 was less successful. The addition of platinum caused severe decrease of pore ordering as compared to the toluene-free system, and only one reflection at a low angle could be observed in X-ray diffractograms. Even for S-1 with only 1 mL of platinum/toluene solution added, the (110) and (200) reflections of the hexagonal structure were not observed. However, the position of the (100) peak was shifted to lower 2θ values, if the precursor solution was added. The specific surface area (S-2, 824 m^2 g^{-1}; S-1, 825 m^2 g^{-1}) was comparable to that of pure SBA-15 (S-0, 786 m^2 g^{-1}). The lower incorporation can be attributed to the extended time needed for the synthesis of SBA-15 (28 h), as compared to the synthesis of platinum containing MCM-41 (1 h). The long time required for SBA-15 synthesis allows the $Pt(acac)_2$ precursor to diffuse from the toluene to the ethanol/water mixture resulting from TEOS hydrolysis. A platinum incorporation of 48% for sample S-1 and 59% for S-2 was achieved. However, the surface areas of these materials are high (Table 2) and comparable to those of pure SBA-15. On the other hand, nitrogen adsorption isotherms (Supporting Information) of platinum containing samples show hysteresis loops which are much broader than in the case of Pt-free SBA-15 (S-0). The latter may be the effect of pore blocking by Pt particles or of the structural changes (due to the presence of swelling agent) in the SBA-15, leading to the formation of a bottleneck-like pore geometry.

Pt-Catalyzed Template Removal. For a Pt-free MCM-41 material, typically the surfactant is removed by calcination at a temperature of 540 °C[1,29] (Scheme 1, step 3). Other template removal procedures are known[38] such as solvent extraction[39,40] or ozone treatment[41] but often complete removal is not achieved. The calcination behavior critically depends on parameters such as the surfactant chain length, the type of oxide phase, and the atmosphere.[23,42] According to TG/MS and differential scanning calorimetry measurements in air, three steps can be distinguished.[23,24] In the first decomposition step, at temperatures between 150 and 250 °C, Hofmann degradation of the template into trimethylamine and hexadecane occurs. In the range of 250 and 300 °C exothermic cracking of the long chain hydrocarbons takes place followed by oxidation at temperatures exceeding 320 °C. Typically, the template removal is stopped at 550 °C.

(34) Abis, L.; Dell' Amico, D. B.; Busetto, C.; Calderazzo, F.; Caminiti, R.; Ciofi, C.; Garbassi, F.; Masciarelli, G. *J. Mater. Chem.* **1998**, *8*, 751−759.
(35) Reddy, K. M.; Moudrakovski, I.; Sayari, A. *J. Chem. Soc., Chem. Commun.* **1994**, 1059−1060.
(36) Reddy, J. S.; Liu, P.; Sayari, A. *Appl. Catal., A* **1996**, *148*, 7−21.
(37) Chao, K. J.; Wu, C. N.; Chang, H.; Lee, L. J.; Hu, S. F. *J. Phys. Chem. B* **1997**, *101*, 6341−6349.
(38) Patarin, J. *Angew. Chem., Int. Ed.* **2004**, *43*, 3878−3880.
(39) Huang, Z.; Huang, L.; Shen, S. C.; Poh, C. C.; Hidajat, K.; Kawi, S.; Ng, S. C. *Microporous Mesoporous Mater.* **2005**, *80*, 157−163.
(40) Gornes, W. A.; Cardoso, L. A. M.; Gonzaga, A. R. E.; Aguiar, L. G.; Andrade, H. M. C. *Mater. Chem. Phys.* **2005**, *93*, 133−137.
(41) Parikh, A. N.; Navrotsky, A.; Li, Q. H.; Yee, C. K.; Amweg, M. L.; Corma, A. *Microporous Mesoporous Mater.* **2004**, *76*, 17−22.
(42) Kleitz, F.; Schmidt, W.; Schüth, F. *Microporous Mesoporous Mater.* **2001**, *44*, 95−109.

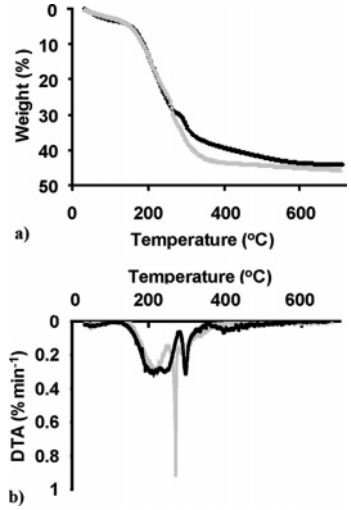

Figure 4. TG (a) and differential TG (b) calcination curves of pure MCM-41 (M-0, black) and 2 wt % platinum containing MCM-41 (M-4, gray) in air.

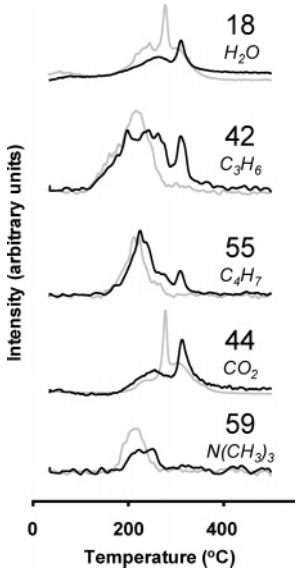

Figure 5. Combustion products detected by mass spectrometry during the TG measurements in air as a function of temperature. Black lines correspond to the M-0 (pure MCM-41), and gray curves correspond to the M-4 (with 2 wt % Pt) sample. Numbers indicate the *m*/*z* ratio of species evolved and the corresponding product.

Comparing the calcination process for M-0 and M-4 (Figure 4a,b), the removal of the template in the platinum-containing sample starts at the same temperature as for the platinum-free material, but complete removal is achieved at significantly lower temperatures (400 °C) as compared to M-0 (550 °C). Also the species evolving during the heat treatment are released at different temperatures. Fragments resulting from cracking of the large chain hydrocarbons are released up to 350 °C[23] (C_3H_6, $m/z = 42$; C_4H_7, $m/z = 55$). This is also observed in case of the M-0 sample (Figure 5). One or two broad overlapping peaks are present on $m/z = 42$ and 55 between 150 and 290 °C, and one is centered at 320 °C. The latter was observed for all cracking products in case of all surfactant hydrocarbon chain lengths.[23] However, in case of platinum-containing material (M-4) only one peak between 150 and 260 °C is present (Figure 5, $m/z = 55$, 42]. On the other hand at 270 °C large amounts of CO_2 ($m/z = 44$) are evolved as compared to M-0, suggesting that the cracking products were immediately oxidized by the integrated platinum catalyst to form CO_2 or direct oxidation of long chain alkanes took place. Also H_2O formation increases at this temperature. The TG/MS experiments show that platinum, located inside the pores, acts as an oxidation catalyst. The lower calcination temperatures are feasible because of the presence of the Pt particles and could provide a new way for the manufacture of mesoporous transition metal oxides that often tend to collapse at higher temperatures as a result of crystallization processes or low melting temperatures. The method could also improve the preparation of mesoporous silica films because of the decrease of stress and strain between the substrate and the porous silica layer developing in the calcination process. However, in the case of silica, low calcination temperatures may result in the lower densification of silica and subsequently lower hydrothermal stability.

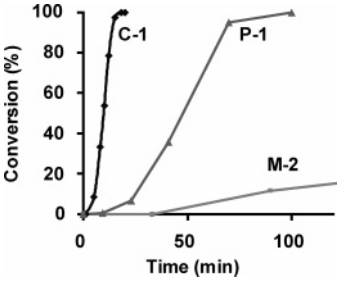

Figure 6. Catalytic conversion of cinnamic acid under heterogeneous conditions. Samples containing platinum (M-2, 1 wt %) and palladium (P-1, 0.3 wt %) were compared to commercially available (C-1) 5 wt % palladium supported on a carbon catalyst.

Scheme 2. Hydrogenation of Cinnamic Acid

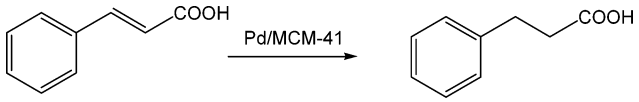

Catalytic Properties: Hydrogenation of Cinnamic Acid. Hydrogen chemisorption studies on in situ synthesized Pt/MCM-41 demonstrated the principle accessibility of the platinum inside the mesoporous channels. A metal dispersion (fraction of active surface metal atoms) of 24% was measured for M-2 with 1 wt % Pt loading. Further catalytic characterization was performed using a model hydrogenation reaction of cinnamic acid to hydrocinnamic acid under heterogeneous conditions (Scheme 2). After 90 min of reaction, the platinum containing MCM-41 (M-2) showed 16% conversion and 100% selectivity toward hydrocinnamic acid (Figure 6). The time required for full conversion was 660 min. However, in the case of the Pd/MCM-41 catalyst (P-1, Table 2) this reaction was much faster, and after the same time (90 min) 100% conversion of the acid was observed (with 100% selectivity). In comparison, a commercially available catalyst (5 wt % palladium supported on carbon, C-1), showed full conversion (with 100% selectivity) already after 18 min, but in the latter case the metal loading was also 16 times higher than in the case of P-1. A blank experiment carried out without catalyst showed no conversion, even after 1 day of hydrogen treatment. The highest specific reaction rate was observed for Pd/MCM-41 (P-1, 0.70 mmol g^{-1} s^{-1}) and was significantly higher than that

for the commercial C-1 catalyst (5 wt % Pd/carbon, 0.21 mmol g^{-1} s^{-1}). For the platinum containing sample M-1 a lower specific reaction rate was observed (0.05 mmol g^{-1} s^{-1}) as compared to both palladium catalysts.

Conclusions

Summarizing, we have presented a one-step, in situ preparation procedure of platinum-containing MCM-41. The highly porous material shows well-dispersed platinum metal predominately confined inside the pores of the mesoporous silica. Particles outside the pore system were not detected using TEM. The confined Pt particles catalyze the removal of surfactant from the MCM-41 and allow calcination at lower temperatures. A high catalytic activity was observed in the hydrogenation of cinnamic acid under heterogeneous conditions. The in situ method presented can be widely applied for incorporation of other metals or oxides into MCM-41 and large pore silica such as SBA-15. Moreover, this method can be easily applied for other metal/mesoporous oxide systems because no interaction between metal oxide and platinum precursor exists during the synthesis.

Acknowledgment. The authors would like to thank Prof. H. Lichte and Dr. M. Lehmann for their support of the TEM investigations at the Triebenberg Laboratory and Dr. C. Weidenthaler at the Max-Planck-Institut für Kohlenforschung in Mülheim an der Ruhr for the XPS measurement.

Supporting Information Available: XPS spectra of the M-2 sample and nitrogen physisorption isotherms and BJH pore size distrubutions of pure MCM-41 (M-2) and Pt/MCM-41 (M-4) samples and SBA-15 and Pt/SBA-15 samples with different metal loadings. This material is available free of charge via the Internet at http://pubs.acs.org.

CM052830N